PHYSICAL REVIEW C
NUCLEAR PHYSICS

THIRD SERIES, VOLUME 45, NUMBER 5 MAY 1992

PHYSICAL REVIEW C VOLUME 45, NUMBER 5 MAY 1992

Hard photon production in proton-deuteron reactions at intermediate energies

K. Nakayama
Institut für Kernphysik, Forschungszentrum Jülich, D-5170 Jülich, Germany
and Department of Physics and Astronomy, University of Georgia, Athens, Georgia 30602
(Received 20 September 1991)

Energetic photon production cross sections in proton-deuteron reactions at intermediate proton incident energies are calculated by using a meson-exchange potential model for describing the elementary nucleon-nucleon bremsstrahlung amplitude. The convection, magnetization, and exchange current contributions as well as the kinematics prescribed by the momentum distribution of the deuteron are included explicitly. The results are compared with the recent data of the Grenoble and Michigan State groups. The absolute cross sections are consistently underpredicted by $\sim(20-40)\%$ which indicates that further work is required for a better understanding of the elementary *pn* bremsstrahlung process.

PACS number(s): 25.20.Lj, 25.10.+s

There has been a resurgence of interest in proton-neutron (*pn*) bremsstrahlung reactions since the first observation of energetic photons produced in heavy-ion collisions at intermediate energies was reported a few years ago [1–4]. Theoretical models [5–8] using transport equations to describe the heavy-ion dynamics require the elementary *pn* bremsstrahlung process as the basic ingredient for describing the photon production in these heavy-ion collisions. However, due to experimental difficulties, *pn* bremsstrahlung data are far too sparse to provide the necessary information required in heavy-ion calculations. Consequently, these calculations have to rely on theoretical predictions of the elementary *pn* bremsstrahlung process. Indeed, to our knowledge, there are only four reports of *pn* bremsstrahlung data [9–12] in the early literature and two more recent reports, one by Dupont *et al.* [13] at $T_{\rm lab}=76$ MeV incident energy and another by Malek *et al.* [14] at $T_{\rm lab}=170$ MeV. Most of these data were taken under quite restricted kinematical conditions. Furthermore, the data by Brady *et al.* [12] were taken under kinematical conditions which are very different from those required for interpreting existing heavy-ion data. The data by Koehler *et al.* [11] and by Edgington and Rose [9] are deduced from the proton-deuteron (*pd*) bremsstrahlung reaction. Moreover, there is some evidence that the data of Ref. [9] may suffer from a systematic error [11,15–18]. In an effort to provide reliable input for calculations of heavy-ion photoproduction, the *pn* bremsstrahlung process based on meson-exchange models has been investigated theoretically [16,17]. The calculations of Ref. [16] and [17] have been compared with an earlier calculation of Brown and Franklin [19] and are in excellent agreement, provided the bremsstrahlung amplitude of Ref. [19] is multiplied by a factor of $\sqrt{m/\varepsilon'}\sqrt{m/\varepsilon}$ which is required to satisfy the relativistic unitary condition of the nonrelativistically constructed S matrix [17,20]. The correction to the *pn* bremsstrahlung cross sections due to the factor mentioned above is, however, of the order of 10% at most at a nucleon incident energy of $T_{\rm lab}=200$ MeV. Although the present type of calculations of *pn* bremsstrahlung are in reasonable agreement with the limited data of Brady *et al.* [12] and of Koehler *et al.* [11] [these data involve uncertainties of $\sim\pm(20-50)\%$], there is a tendency of these calculations to underpredict the measured cross sections.

Quite recently, *pd* bremsstrahlung cross sections have been measured at a proton incident energy of $T_{\rm lab}=200$ MeV by the Grenoble group [21] and at $T_{\rm lab}=145$ and 195 MeV by the Michigan State group [22] under kinematical conditions appropriate for understanding of the *pn* bremsstrahlung process as it enters the calculation of energetic photon production in heavy-ion collisions. Although the *pd* bremsstrahlung process is different from the pure *pn* bremsstrahlung process, it is much easier to measure experimentally than the latter process and offers an important alternative for testing theoretical models of *pn* bremsstrahlung reactions. In the present work we calculate, for the first time, *pd* bremsstrahlung cross sections using modern meson-exchange potential models and compare the results with the data mentioned above.

The formalism for calculating *pd* bremsstrahlung is basically the same as given in Refs. [16] and [23]. We express the photon emission probability per unit solid angle and unit photon energy as

$$\frac{d^2P_{pd\gamma}}{d\omega\, d\Omega}=\frac{1}{W_{NN}}\frac{d^2W_{pd\gamma}}{d\omega\, d\Omega}\ , \tag{1}$$

where $d^2W_{pd\gamma}/d\omega\, d\Omega$ denotes the pd bremsstrahlung differential transition rate and W_{NN} is the total nucleon-nucleon collisional rate irrespective of the bremsstrahlung process.

We calculate the pd bremsstrahlung transition rate by simply folding the elementary NN bremsstrahlung transition rate with the momentum distribution function of the nucleons in the target deuteron:

$$\begin{aligned}\frac{d^2W_{pd\gamma}}{d\omega\, d\Omega}=\frac{1}{\varepsilon_1}\int\frac{d^3p_2}{(2\pi)^3\varepsilon_2}n(\mathbf{p}_2)2\pi\omega\int\frac{d^3p_1'}{(2\pi)^3\varepsilon_1'}\frac{d^3p_2'}{(2\pi)^3\varepsilon_1'}Q\\ \times\left\{\frac{1}{4}\sum_{\substack{SM_S\\ S'M_{S'}}}\sum_{\epsilon}|\sqrt{\varepsilon_1'\varepsilon_2'\omega}\langle\epsilon,\mathbf{k};\mathbf{p}_1',\mathbf{p}_2',S'M_{S'}|V_{em}|0;\mathbf{p}_1,\mathbf{p}_2,SM_S\rangle\sqrt{\varepsilon_1\varepsilon_2}|^2\right\}\\ \times\delta^3(\mathbf{p}_1+\mathbf{p}_2-\mathbf{p}_1'-\mathbf{p}_2'-\mathbf{k})\delta(\varepsilon_1+\varepsilon_2-\varepsilon_1'-\varepsilon_2'-\omega)\ .\end{aligned} \tag{2}$$

In the above equation, the primed (unprimed) quantities refer to the final (initial) two interacting nucleons' energies $\varepsilon_1',\varepsilon_2'$ ($\varepsilon_1,\varepsilon_2$), momenta $\mathbf{p}_1',\mathbf{p}_2'$ ($\mathbf{p}_1,\mathbf{p}_2$), total spin S' (S), and spin projection $M_{S'}$ (M_S). The matrix element in curly brackets denotes the photon emission amplitude for a photon with polarization ϵ and momentum $\mathbf{k}$; ω stands for the photon energy. The momentum distribution function of the nucleons inside the target deuteron is denoted by n and Q is the Pauli blocking operator which prevents nucleons in the final state from having the same momenta.

Analogously, the total NN collisional rate is given by

$$\begin{aligned}W_{NN}=\frac{1}{\varepsilon_1}\int\frac{d^3p_2}{(2\pi)^3\varepsilon_2}n(\mathbf{p}_2)\int\frac{d^3p_1'}{(2\pi)^3\varepsilon_1'}\frac{d^3p_2'}{(2\pi)^3\varepsilon_2'}Q\left\{\frac{1}{4}\sum_{\substack{SM_S\\ S'M_{S'}}}|\sqrt{\varepsilon_1'\varepsilon_2'}\langle\mathbf{p}_1',\mathbf{p}_2',S'M_{S'}|T|\mathbf{p}_1,\mathbf{p}_2,SM_S\rangle\sqrt{\varepsilon_1\varepsilon_2}|^2\right\}\\ \times(2\pi)^4\delta^3(\mathbf{p}_1+\mathbf{p}_2-\mathbf{p}_1'-\mathbf{p}_2')\delta(\varepsilon_1+\varepsilon_2-\varepsilon_1'-\varepsilon_2')\ ,\end{aligned} \tag{3}$$

where T denotes the NN T matrix associated with the bare NN potential used.

The single-particle energies appearing in Eq. (2) and Eq. (3) are assumed to have the relativistic form

$$\varepsilon(p)=\sqrt{\mathbf{p}^2+m^2}\ , \tag{4}$$

where m stands for the nucleon mass.

The elementary NN bremsstrahlung amplitude has been calculated [16,17] within a meson-exchange potential model where the strongly interacting particles are treated to all orders in perturbation theory while the coupling to the photon is considered only in first order via the minimal substitution in the nonrelativistic nuclear Hamiltonian. The model includes convection, magnetization, as well as important exchange-current contributions. Since the proton-proton (pp) bremsstrahlung process is known to be negligible compared to the pn process [17], we include only the latter mechanism.

The photon cross section is obtained by multiplying the photon emission probability rate given by Eq. (1) by the total pd cross section σ_{pd}:

$$\frac{d^2\sigma}{d\omega\, d\Omega}=\sigma_{pd}\frac{d^2P_{pd\gamma}}{d\omega\, d\Omega}\ . \tag{5}$$

Before comparing our results with the recent data a few remarks are in order. Recently, we have applied a parametrized form of the pn bremsstrahlung amplitude [24] in the description of photon production cross sections in proton-nucleus collisions [23]. The parametrized amplitude is inappropriate for applications to pd bremsstrahlung since in this case, due to much smaller Pauli blocking effects compared to the proton-nucleus case, photon energy regions very near the end point are strongly sampled where the parametrized amplitude is inaccurate.

The importance of considering the phase-space distribution of the nucleon inside the deuteron in the pd bremsstrahlung calculation is illustrated in Fig. 1, where the pd bremsstrahlung cross section (solid curve) is compared to the elementary pn bremsstrahlung cross section (dashed curve) at a proton incident energy of $T_{\rm lab}=200$ MeV and for a fixed photon emission angle of $\theta=90°$. For the pd total cross section we use the experimental value of $\sigma_{pd}=61\pm4$ mb at $T_{\rm lab}=208$ MeV [25]. We see that the pd and pn bremsstrahlung cross sections are practically the same for photon energies up to $\omega\sim70$ MeV. For higher photon energies, however, these cross sections behave quite differently. In the elementary pn bremsstrahlung process, the maximum photon energy allowed by the kinematics is $\omega\sim90$ MeV at $T_{\rm lab}=200$ MeV; however, in the pd bremsstrahlung process at the same incident energy photons with much higher energies can be produced. This is because in pd bremsstrahlung the NN center-of-mass (c.m.) energy involved can be much higher than in elementary pn bremsstrahlung due to the momentum distribution of the nucleon inside the deuteron. In Fig. 1 we have also displayed the recent pd bremsstrahlung cross-section data from the Grenoble group [21] which, together with the theoretical curves, illustrate the importance of an adequate treatment of the phase-space distribution of the nucleon inside the deuteron for describing an energetic photon production process. The results in Fig. 1 also indicate clearly that the

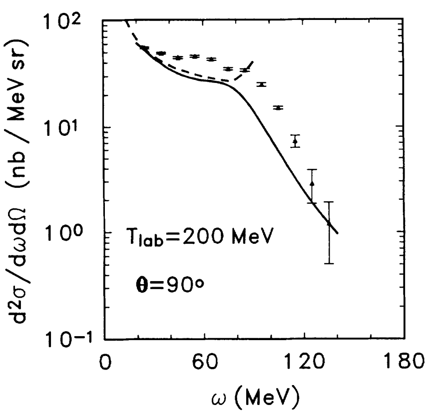

FIG. 1. Proton-deuteron bremsstrahlung cross section (solid line) in the laboratory frame as a function of photon energy ω at a proton incident energy of $T_{\rm lab}=200$ MeV and photon emission angle of $\theta=90°$. An experimental value of $\sigma_{pd}=61\pm4$ mb [25] for the *pd* total cross section is used. The dashed line represents the corresponding elementary *pn* bremsstrahlung result. The data are from Ref. [21].

present *pd* bremsstrahlung calculations underestimates the data. This and other features of the present calculation will be discussed later with more systematics. The *pn* bremsstrahlung calculation accompanying the *pd* bremsstrahlung data in Ref. [21] has been taken from Fig. 3 of Ref. [17] and differs from the present calculated *pn* bremsstrahlung cross section shown in Fig. 1 because the result in Ref. [17] corresponds to photons emitted at $\theta=90°$ in the *pn* c.m. frame (cross section in the *pn* c.m. frame), while the present result is calculated in the laboratory frame in order to compare directly with *pd* bremsstrahlung results. In particular, the *pn* bremsstrahlung cross section in the laboratory frame at $\theta=90°$ is reduced with respect to the corresponding cross section in the *pn* c.m. frame since it is more forward peaked in the laboratory frame than in the c.m. frame. We note that the *pn* bremsstrahlung cross section has roughly a dipole shape in the c.m. frame [17].

For energetic photons, the calculated results will be sensitive to the phase-space distribution of the nucleon inside the deuteron. In Fig. 2, the product $p^2n(p)$ is shown for two different deuteron wave functions based on *NN* potentials developed by the Bonn group [26,27] which yield deuteron *D*-state probabilities of 4.25% and 5.61%. As can be seen, there is practically no difference between the momentum distributions calculated from these potentials for nucleon momenta up to ~1.5 fm^{-1} since the *S*-state wave function is well determined, not only for the potentials considered here, but also for most realistic potentials in the literature. The difference we see around $p\sim3$ fm^{-1} is due to the difference in the *D*-state wave function between the two potentials, which is reflected in different *D*-state probabilities. The *pd* bremsstrahlung reaction is primarily sensitive to the momentum distribution up to $p\sim1$ fm^{-1} and cannot probe the relatively large differences at larger *p* because the cross section becomes negligibly small for larger bound state momentum *p*.

We now compare our results with the data. Figure 3 shows the results for *pd* bremsstrahlung cross sections as a function of $\omega/T_{\rm lab}$ at a proton incident energy near $T_{\rm lab}=200$ MeV and for three photon emission angles of $\theta=60°$, 90°, and 120°. For the *pd* total cross section we use the experimental value of $\sigma_{pd}=61\pm4$ mb at $T_{\rm lab}=208$ MeV [25]. The data at an incident energy of $T_{\rm lab}=200$ MeV (triangle) are from the Grenoble group [21]; the $T_{\rm lab}=195$ MeV data (circle) are from the Michigan State group [22]. The 200 MeV data from Ref. [21] are corrected for photons produced via π_0 decay and for radiactive capture by the deuterium; however, these corrections are small. The present theoretical calculations do not account for these contributions. The data from the Michigan State group [22] are uncertain to within at least $\pm25\%$ in absolute value [28]. First of all, the figure illustrates the level of agreement between the data from the two groups. At the photon emission angle of $\theta=90°$, the agreement is excellent. At $\theta=120°$ the agreement is reasonable, but at $\theta=60°$ there is clear

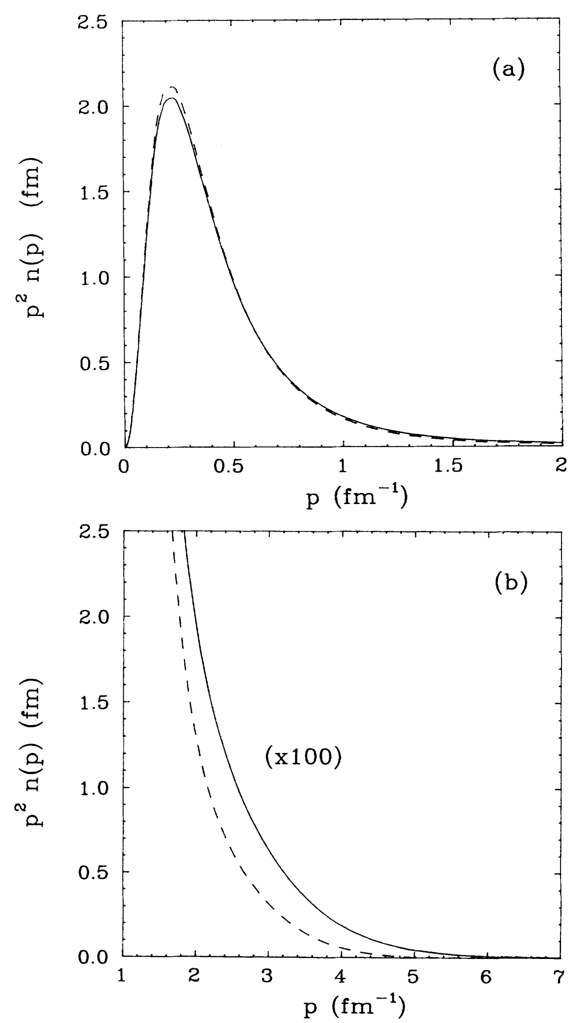

FIG. 2. The product $p^2n(p)$ [with $n(p)$ denoting the single-particle momentum distribution function in the deuteron] as a function of nucleon momentum *p*. The solid line corresponds to the full Bonn potential [26] with a *D*-state probability of 4.25%, while the dashed line corresponds to the Bonn C potential [27] with a *D*-state probability of 5.61%.

disagreement between the data for $\omega/T_{\rm lab}<0.25$ which corresponds to photon energies below $\omega\sim 50$ MeV. With the exception of the $\theta=90°$ case, we also note that the data from the Grenoble group [21] are systematically lower than those from the Michigan State group [22] for $\omega/T_{\rm lab}<0.4$ corresponding to $\omega<80$ MeV, approximately. Now we see that, overall, the theory underestimates the measured cross sections. This is particularly clear for the photon emission angle of $\theta=90°$, where the data are very accurate; the underprediction is about 40%. At

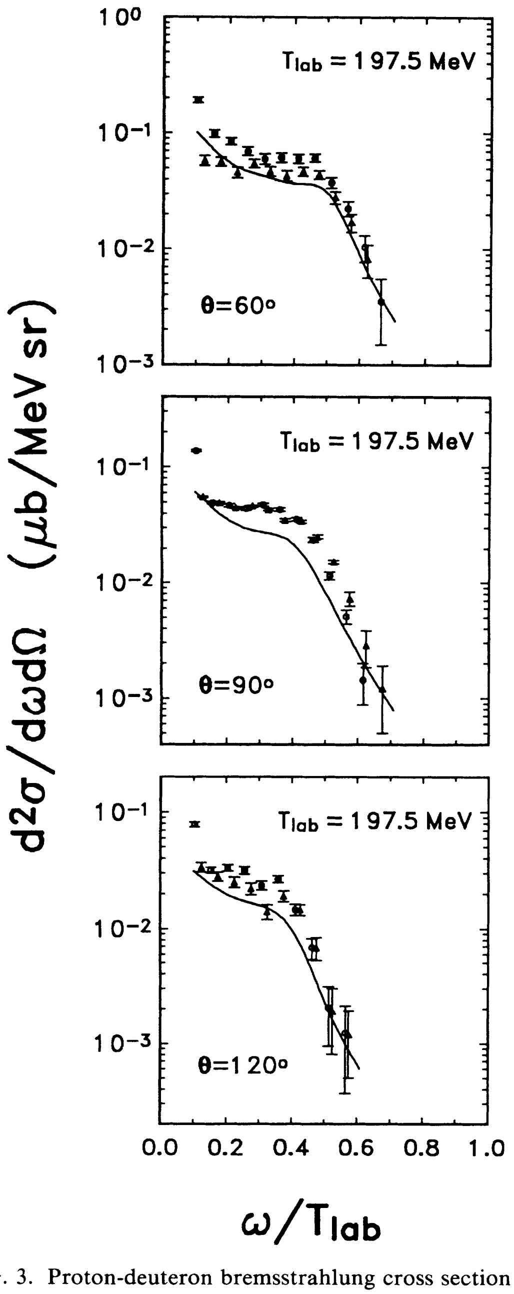

FIG. 3. Proton-deuteron bremsstrahlung cross section in the laboratory frame as a function of $\omega/T_{\rm lab}$ at an average proton incident energy of $T_{\rm lab}=197.5$ MeV and for three photon emission angles of $\theta=60°$, 90°, and 120°. An experimental value of $\sigma_{pd}=61\pm4$ mb [25] for the *pd* total cross section is used. The data are from Ref. [21] at a proton incident energy of $T_{\rm lab}=200$ MeV (triangle) and from Ref. [22] at $T_{\rm lab}=195$ MeV (circle).

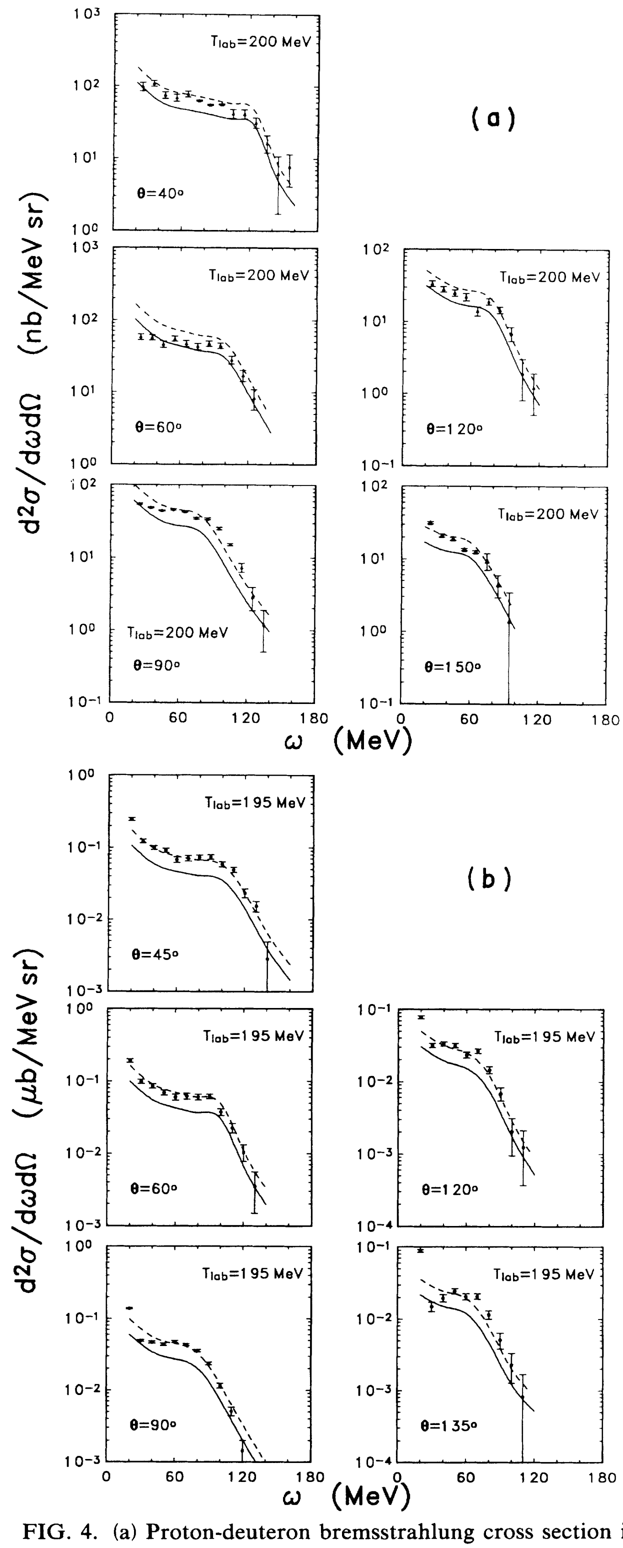

FIG. 4. (a) Proton-deuteron bremsstrahlung cross section in the laboratory frame as a function of photon energy ω at a proton incident energy of $T_{\rm lab}=200$ MeV and for various photon emission angles θ. An experimental value of $\sigma_{pd}=61\pm4$ mb [25] for the *pd* total cross section is used. The solid lines correspond to the present prediction, while the dashed lines correspond to the present results *multiplied by an arbitrary normalization factor* of $N=1.67$. The data are from Ref. [21]. (b) Same as (a) for a proton incident energy of $T_{\rm lab}=195$ MeV. The data are from Ref. [22].

$\theta = 120°$, the theory yields cross sections that are roughly 30% smaller than the data. At the photon emission angle of $\theta = 60°$, the calculated results are closer to the Grenoble data than to the Michigan State data; the latter are underestimated by $\sim 40\%$. However, as is better illustrated in Fig. 4, the calculated shapes of both the energy and angular distributions agree much better with the Michigan State data than with the Grenoble data.

Since the Grenoble [21] and Michigan State [22] groups have also reported *pd* bremsstrahlung cross sections at photon emission angles which differ from each other, we now compare these data separately with the corresponding theoretical results. For completeness we also include the cases shown in Fig. 3. The difference of 5 MeV in the proton incident energies between the data from the Grenoble and Michigan State groups is taken into account in the calculated results. However, this small energy difference affects the calculated results only for photons near the end-point energy where the uncertainties in the data are large.

Figure 4(a) shows the results for *pd* bremsstrahlung cross sections (solid curves) as a function of photon energy at a proton incident energy of $T_{\rm lab} = 200$ MeV and for various photon emission angles. The theory underestimates the data by $\sim (30-40)\%$ depending on the photon emission angle, except for a photon emission angle of $\theta = 60°$ where the prediction is much closer to the data than at other angles. As we have seen in Fig. 3, however, the uncertainty in the data at this photon emission angle is much larger than at other angles in the sense that there is considerable disagreement with the corresponding data from the Michigan State group [22], especially in the low photon energy region where the theory even overestimates the measured cross sections of Ref. [21]. In order to assess the level of agreement/disagreement between the calculated and measured cross sections more easily, we also show the theoretical results multiplied by an *arbitrary normalization factor* of $N = 1.67$ (dashed curves). Although absolute cross sections are underpredicted, the overall agreement of the shape of both the energy and angular distributions with the data is comparable to that obtained for proton-nucleus bremsstrahlung [23], except again for $\theta = 60°$. In Fig. 4(b) a comparison with the data of Clayton [22] is shown for a proton incident energy of $T_{\rm lab} = 195$ MeV. We use the same experimental value of $\sigma_{pd} = 61 \pm 4$ mb for the *pd* total cross section. The solid and dashed curves correspond to the unnormalized and normalized [with the normalization factor of $N = 1.67$ as in Fig. 4(a)] results, respectively. Similar features to those observed in Fig. 4(a) can be seen; the cross sections are underpredicted by $\sim 40\%$. The *shapes* of both the energy and angular distributions are much better reproduced than in the case of the $T_{\rm lab} = 200$ MeV data in Fig. 4(a). The underprediction of the relatively accurate *pd* bremsstrahlung cross sections by $\sim (30-40)\%$ observed in Fig. 4, which is consistent with similar results obtained for the elementary *pn* bremsstrahlung reaction [16,17], strongly suggests that some significant contribution to the elementary *pn* bremsstrahlung process is still not taken into account. It is, however, difficult to think of a process(es) which might give such a significant contribution, at least in the *NN* c.m. energy domain involved in the present calculations. The only obvious term which has been left out of the present calculation is the relativistic spin correction. This correction is known to reduce the cross section considerably in *pp* bremsstrahlung [29,30]; if the inclusion of this term should also reduce the *pn* bremsstrahlung cross section, this would further increase the discrepancy with the existing data.

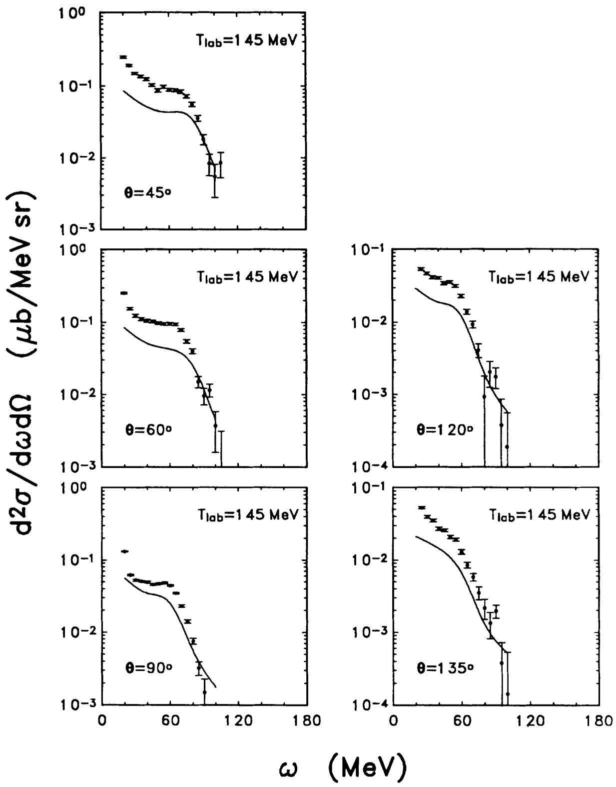

FIG. 5. Same as Fig. 4(a) for a proton incident energy of $T_{\rm lab} = 145$ MeV. The data are from Ref. [22].

The results at a lower incident energy of $T_{\rm lab} = 145$ MeV are shown in Fig. 5 together with the data from Ref. [22]. At this energy no *pd* total cross-section data are available. An estimate using the *pn* and *pp* total cross sections at $T_{\rm lab} = 145$ MeV incident energy in an eikonal model yields $\sigma_{pd} \sim 70$ mb. This value of σ_{pd} yields the *pd* bremsstrahlung cross sections which are in good agreement (similar to that shown in Fig. 1) with the calculated *pn* bremsstrahlung results for low energy photons. We see that the cross sections are underestimated more in the low photon energy region, especially at forward photon emission angles. As a result the shape of the calculated cross section (without the renormalization) is seen to be in significantly poorer agreement with the data than near $T_{\rm lab} = 200$ MeV. Unlike heavier systems, where multistep contributions can be significant in the low photon energy region, such a discrepancy is not easily understood in *pd* bremsstrahlung.

In summary, we have investigated the production of hard photons in intermediate energy *pd* reactions. Absolute cross sections are underpredicted by $\sim (20-40)\%$ which is consistent with the results obtained for the *pn* bremsstrahlung reaction and suggests that further work is needed for a better understanding of the elementary *pn* bremsstrahlung process. This underprediction of the *pn* bremsstrahlung cross section should be considered when applying our *pn* bremsstrahlung calculation to the description of more complicated processes. As far as the shapes of both the energy and angular distributions are concerned, the agreement with the recent data from the Michigan State group [22] at $T_{\rm lab}=195$ MeV is better than the agreement with the data from the Grenoble group [21] at $T_{\rm lab}=200$ MeV. At $T_{\rm lab}=145$ MeV incident energy, the present model underestimates the cross section more in the low photon energy region than in high energy region. This kind of discrepancy is not easy to understand since, for *pd* bremsstrahlung, we do not expect secondary collisions to play a significant role. It would be interesting to have *pd* bremsstrahlung data at lower proton incident energies in order to see whether the discrepancy increases or decreases at lower energies. This could provide helpful insight as to the origin of the disagreement.

ACKNOWLEDGMENTS

We would like to thank J. Pinston and J. Clayton for providing us with their data prior to publication. We also thank W. G. Love for many discussions and for a careful reading of the manuscript. This work was supported in part by the NATO Grant No. RG85/0093.

[1] E. Grosse, P. Grimm, H. Heckwolf, W. F. J. Mueller, H. Noll, A. Oskarsson, H. Stelzer, and W. Roesch, Europhys. Lett. **2**, 9 (1986).
[2] J. Stevenson *et al.*, Phys. Rev. Lett. **57**, 555 (1986).
[3] N. Alamanos, P. Braun-Munzinger, R. H. Freifelder, P. Paul, J. Stachel, T. C. Awes, R. L. Fergusson, F. E. Obenshain, F. Plasil, and G. R. Young, Phys. Lett. B **173**, 392 (1986).
[4] K. Kwato Njock, M. Maurel, E. Monnand, H. Nifenecker, J. A. Pinston, F. Schussler, and D. Barneoud, Phys. Lett. B **175**, 125 (1986).
[5] T. S. Biro, K. Niita, A. A. DePaoli, W. Bauer, W. Cassing, and U. Mosel, Nucl. Phys. **A475**, 579 (1987).
[6] B. A. Remington, M. Blann, and G. F. Bertsch, Phys. Rev. C **35**, 1720 (1987).
[7] C. M. Ko and J. Aichelin, Phys. Rev. C **35**, 1976 (1987).
[8] R. Heuer, B. Müller, H. Stoecker, and W. Greiner, Z. Phys. A **330**, 315 (1988).
[9] J. Edgington and B. Rose, Nucl. Phys. **89**, 523 (1966).
[10] K. W. Rothe, P. F. M. Koehler, and E. H. Thorndike, Phys. Rev. **157**, 1247 (1966).
[11] P. F. M. Koehler, K. W. Rothe, and E. H. Thorndike, Phys. Rev. Lett. **18**, 933 (1967).
[12] F. P. Brady and J. C. Young, Phys. Rev. C **2**, 1579 (1970); *ibid.* **7**, 1707 (1973).
[13] C. Dupont, C. Deom, P. Leleux, P. Lipnik, P. Macq, A. Ninane, J. Pestineau, S. W. Kitwanga, and P. Wauters, Nucl. Phys. **A481**, 424 (1988).
[14] F. Malek, H. Nifenecker, J. A. Pinston, F. Schussler, S. Drissi, and J. Julien, Phys. Lett. B **266**, 255 (1991).
[15] H. Nifenecker and J. A. Pinston, Annu. Rev. Nucl. Part. Sci. **40**, 113 (1990).
[16] K. Nakayama, Phys. Rev. C **39**, 1475 (1989).
[17] V. Herrmann, J. Speth, and K. Nakayama, Phys. Rev. C **43**, 394 (1991).
[18] H. Nifenecker, M. Kwato Njock, and J. A. Pinston, Nucl. Phys. **A495**, 3c (1989).
[19] V. R. Brown and J. Franklin, Phys. Rev. C **8**, 1706 (1973).
[20] V. Herrmann and K. Nakayama (in preparation).
[21] J. A. Pinston, D. Barneoud, V. Bellini, S. Drissi, J. Guillot, J. Julien, H. Nifenecker, and F. Schussler, Phys. Lett. B **249**, 402 (1990).
[22] J. Clayton, W. Benenson, M. Cronqvist, R. Fox, D. Krofchek, R. Pfaff, T. Reposeur, J. D. Stevenson, J. S. Winfield, and B. Young, Phys. Rev. C **45**, 1810 (1992).
[23] K. Nakayama and G. F. Bertsch, Phys. Rev. C **40**, 2520 (1989).
[24] K. Nakayama and G. F. Bertsch, Phys. Rev. C **40**, 685 (1989).
[25] H. G. Carvalho, Phys. Rev. **96**, 398 (1954).
[26] R. Machleidt, K. Holinde, and Ch. Elster, Phys. Rep. **149**, 1 (1987).
[27] R. Machleidt, Adv. Nucl. Phys. **19**, 189 (1989).
[28] W. Benenson (private communication).
[29] L. S. Celenza *et al.*, Phys. Lett. **41B**, 283 (1972).
[30] R. L. Workman and H. W. Fearing, Phys. Rev. C **34**, 780 (1986).